

# Surface modification of resistance welding electrode by electro-spark deposited composite coatings: Part I. Coating characterization

Zheng Chen<sup>a,\*</sup>, Y. Zhou<sup>b</sup>

<sup>a</sup> Department of Materials Science and Engineering, Jiangsu University of Science and Technology, Zhenjiang, 212003, PR China

<sup>b</sup> Department of Mechanical Engineering, University of Waterloo, 200 University Avenue West, Waterloo, Ontario, Canada N2L 3G1

Received 21 October 2005; accepted in revised form 9 February 2006

Available online 31 March 2006

## Abstract

To improve electrode life during resistance spot welding of Zn-coated steel sheets, a monolithic TiC<sub>p</sub>/Ni composite coating was deposited onto the surface of a Cu–Cr–Zr electrode by an electro-spark deposition process. The coating was designed as a barrier to prevent electrodes from alloying with the Zn-coating leading to degradation by pitting or erosion. Some coated electrodes were also subjected to laser treatment in order to eliminate cracks formed in the as-coated monolithic TiC<sub>p</sub>/Ni composite coating. In addition, a multi-layer deposition process has also been proposed to improve the coating quality by using Ni and TiC<sub>p</sub>/Ni composite as deposition materials alternately. The microstructure and mechanical properties of the coatings have been characterized by scanning electron microscopy, energy dispersive X-ray analysis, X-ray diffraction and micro-hardness tests. The results showed that extensive cracking occurred within the monolithic TiC<sub>p</sub>/Ni coating and at the interface. It was found possible to reduce or eliminate cracks and delamination of the monolithic TiC<sub>p</sub>/Ni coating via the multi-layer deposition process using Ni, TiC<sub>p</sub>/Ni. The multi-layer coatings of Ni/(TiC<sub>p</sub>/Ni)/Ni showed higher Ni content and lower hardness. Although post laser treatment of monolithic TiC<sub>p</sub>/Ni coatings could eliminate cracks and improve coating quality, the softening of the copper alloy substrate limited the performance of laser treated electrodes.

© 2006 Elsevier B.V. All rights reserved.

**Keywords:** Electro-spark deposition; Composite; Coating; TiC; Ni; Resistance spot welding; Electrode

## 1. Introduction

Recently the electro-spark deposition (ESD) process has gained increasing interest as a promising surface technique for engineering materials owing to its efficiency, simplicity and cost-effectiveness [1–3]. The ESD is essentially a pulsed-arc microwelding surfacing process that consists of producing periodic electric arcs through a moving conductive electrode (positive pole) energized by a series of capacitors as it is short-circuited momentarily with the base material (negative pole). During the generation of the arc, small particles of the electrode material are melted, accelerated through the arc, impacted against the base metal substrate, solidified rapidly, and build-up occurs incrementally. The duration of the current pulse is typically 1–10 μs with a maximum arc temperature reaching 5000–25,000 K. The pulse time is very short relative to the

interval period, so that very little heat is transferred to the substrate during each cycle. Accordingly, the main advantage associated with the ESD process is that the metallurgically bonded coatings with a strongly adherent interface can be produced with little heat input to the substrate material which remains at or near ambient temperature. This minimizes the changes in microstructure or mechanical properties of the substrate [4–8].

While the ESD has been widely used as a coating process to increase the life of many parts subject to wear [9], corrosion or oxidation [10], it has also been used to coat electrodes in resistance spot welding (RSW) to protect the electrodes from pitting or erosion [11]. It is well known that the electrode life in RSW is considerably shortened when welding Zn-coated steels compared with uncoated steels because of alloying of electrodes with the zinc transferred from the coatings to form brittle brasses [12]. Pitting or erosion occurs during welding due to sticking of electrodes to the workpiece results in the removal of Cu–Zn alloys from the electrode tip, causing accelerated wear

\* Corresponding author. Tel.: +86 511 4401182

E-mail address: [chenz\\_31@yahoo.com.cn](mailto:chenz_31@yahoo.com.cn) (Z. Chen).

Table 1  
Chemical composition of TiC<sub>p</sub>/Ni rod used as deposition materials (wt.%)

Ti	Ni	Co	Mo	W
67	21	2.5	3.0	6.0

Carbon was not detectable by EDX used.

and resulting increased growth of electrode tip diameter [13]. The enlargement of the diameter consequently results in a reduced welding current density (heat generation) and hence an undersized weld between the steel sheets [14].

To prevent the RSW electrode from alloying with Zn-coating and pitting or erosion, K. Chan et al. recently reported that a TiC<sub>p</sub>/Ni composite coating deposited on the surface of the Cu–Cr–Zr electrodes by ESD process acted as a barrier to prevent Cu from reacting with Zn and hence improved electrode life [15]. However, this barrier coating of TiC<sub>p</sub>/Ni composite is only temporary during the welding process and is eventually pitted away due to penetration of molten Zn through cracks within the coating and delamination at coating–substrate interface.

In the present work, laser treatment of the as-coated TiC<sub>p</sub>/Ni coating and a multi-layer coating process of Ni, TiC<sub>p</sub>/Ni and Ni have been proposed in order to eliminate cracks formed in monolithic TiC<sub>p</sub>/Ni coatings. The microstructure and mechanical properties of these coatings have been characterized by scanning electron microscopy (SEM), energy dispersive X-ray analysis (EDX), X-ray diffraction (XRD) and micro-hardness tests. Resistance spot welding test will be carried out to examine the performance of the coated electrodes and to investigate metallurgical behavior of deposited coatings in Part II of this work.

## 2. Experimental

Resistance welding electrodes used in the present work were standard B nose domed flat electrodes (5 mm in diameter at top surface). The electrode base metal was precipitation strengthened and cold worked Cu–0.84 wt.% Cr–0.05 wt.% Zr alloy. The roughness of electrodes surface was approximately 2–3 μm. Before commencing the coating experiments, the tip surface of each electrode was cleaned using an acetone rinse. A sintered TiC<sub>p</sub>/Ni composite rod and a commercially pure Ni rod were used to deposit coatings on the surface of electrodes. The

volume percentage of TiC particles (~2 μm in diameter) was around 42 in the composite rod. The chemical composition of TiC<sub>p</sub>/Ni composite rod is listed in Table 1, in which Ni acted as a binder and Mo and W were added to strengthen the hardness and strength of the metal matrix. Deposition of TiC<sub>p</sub>/Ni and Ni coatings was carried out using a laboratory-developed electro-spark deposition machine with a handheld gun in air or argon at room temperature, respectively. The experiment was conducted at a voltage of 40 V and a capacitance of 2000 μF for TiC<sub>p</sub>/Ni deposition and, at a voltage of 5 V and a capacitance of 12,000 μF for deposition of Ni coatings. After deposition, some of the electrodes with monolithic TiC<sub>p</sub>/Ni coating were further treated using a 4 kW diode laser with scanning speed of 80 mm/min in argon. The laser beam has a rectangular shape of 1 × 12 mm and wavelength of 800 nm.

The microstructure and composition of the coating surface and the cross-section were first examined using a JEOL JSM-840 scanning electron microscope (SEM) equipped with energy-dispersive spectrometer (EDS). Phase identification was conducted using a Siemens D500 X-ray diffractometer with Cu K<sub>α</sub> radiation operating at 30 kV and 40 mA. The mechanical behavior was characterized by measuring the micro-hardness of the coating using a MHT 200 microhardness tester with a normal load 100 g applied for 15 s.

## 3. Results and discussion

### 3.1. Microstructure of TiC<sub>p</sub>/Ni coating before and after laser treatment

The topographical features of as-coated monolithic TiC<sub>p</sub>/Ni coating deposited on a Cu–Cr–Zr alloy electrode substrate are shown in Fig. 1. The typical ‘splash’ appearance was a characteristic feature of the ESD technique, especially when air was used for shielding [5]. In the present work, the deposition of TiC<sub>p</sub>/Ni coating was carried out in air. Air established a plasma arc of high thermal conductivity that promotes formation of relatively large molten droplets, i.e., globular mass transfer [5]. In this process the molten droplets are accelerated by the plasma jet, strike the substrate surface at high velocity and splash [2]. It is worth noting that numerous stress relief cracks were visible within the coating. In particular, it was found that cracks formed early in the deposition process

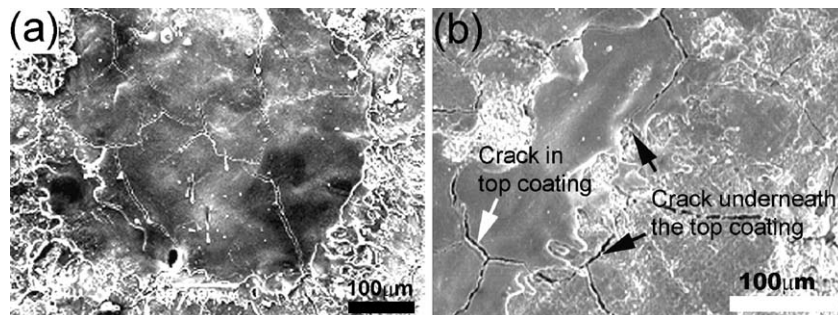


Fig. 1. Surface morphologies of monolithic TiC<sub>p</sub>/Ni coating (a) showing splash appearance and (b) showing cracks underneath the top coating caused cracking of the top coating (as shown by arrows).

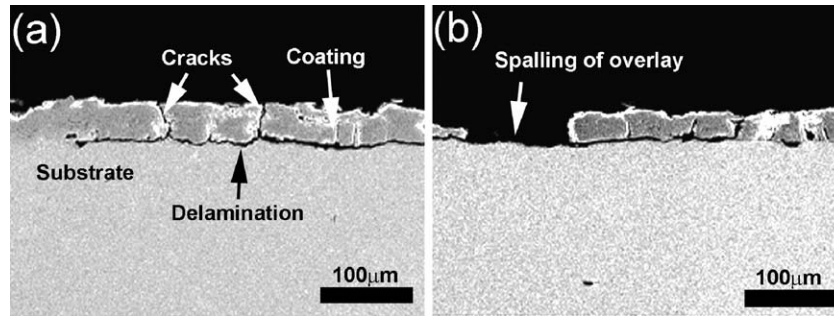


Fig. 2. SEM cross-section images of monolithic  $\text{TiC}_p/\text{Ni}$  coating of (a) cracking within the coating and delamination at the interface and (b) spalling of overlay.

acted as crack nuclei, resulting in progressive upwards propagation to the top layer under tensile stress, as indicated by arrows shown in Fig. 1. Thus, the deposit tended to exist as islands separated by cracks; the average diameter of the islands was estimated to be  $\sim 250 \mu\text{m}$ . The thickness of coating was not uniform, usually from  $30 \mu\text{m}$  to  $40 \mu\text{m}$ , as illustrated in Fig. 2. From cross-section images (Fig. 2), it was observed that when  $\text{TiC}_p/\text{Ni}$  was directly deposited onto copper alloy, some cracks or delamination was seen, not only within the  $\text{TiC}_p/\text{Ni}$  coating, but also at the interface between the substrate and coating. In addition, spalling of  $\text{TiC}_p/\text{Ni}$  coating was observed in some regions due to delamination (as shown by arrow in Fig. 2(b)). Occasionally, a sound and dense interface was formed between the substrate and  $\text{TiC}_p/\text{Ni}$  coating where vertical cracks were still present, as shown in Fig. 3 along with the EDX element maps of Ti, Ni and Cu. Fig. 3 clearly showed the high concentration of Ti within the coating and a sharp interface after deposition. During the deposition process, copper alloy was melted and mixed into the coating, as evidenced by Cu map (Fig. 3). The concentration of Ti, Ni and Cu in the centre area of the coating determined by EDX analysis was averaged from at

least five runs in different regions. As listed in Table 2, the Cu concentration was nearly 17 wt.% in the coating. On the other hand, it was found that a cold extruded copper alloy electrode with the surface roughness of  $2\text{--}3 \mu\text{m}$  was suitable for directly ESD deposition without the needing of subsequent machining or grinding, since the surface of electrode was flat with a large feed value and the coating covered all the surface of electrode.

To observe how the coating cracked during the coating process, the  $\text{TiC}_p/\text{Ni}$  was coated with different times from 0.5 s to 10 s. As shown in Fig. 4(a), after coating with a very short time of 0.5 s, the droplets deposited on the substrate surface were of splash appearance without cracks. The  $\text{TiC}_p/\text{Ni}$  coating began to crack after deposition time of 2 s (Fig. 4(b)), but the cracks were fine, indicating the stress was not high at this time. As coating was continued to 3 s or more, however, many cracks with increased width were observed due to the increased tensile stress (Fig. 4(c, d)). In addition, spalling of the coating was observed (Fig. 4(d)).

The present work showed that direct deposition of  $\text{TiC}_p/\text{Ni}$  onto copper alloy substrate by ESD process caused extensive cracking within the  $\text{TiC}_p/\text{Ni}$  coating and at the coating–

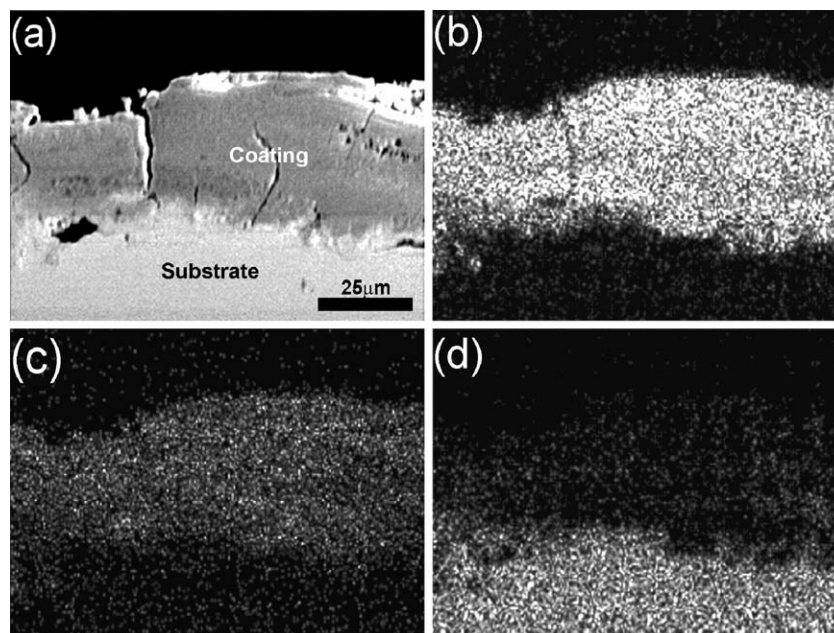


Fig. 3. SEM cross-section images of monolithic  $\text{TiC}_p/\text{Ni}$  coating (a) and corresponding element X-ray mapping of Ti  $\text{K}\alpha$  (b), Ni  $\text{K}\alpha$  (c) and Cu  $\text{K}\alpha$  (d).

Table 2  
Chemical composition (wt.%) and hardness (HV<sub>100</sub>) of the coatings

Coating	Surface			Average in the centre area of the overlays (20 μm × 20 μm)			Hardness
	Ti	Ni	Cu	Ti	Ni	Cu	
TiC <sub>p</sub> /Ni	48.5	20.5	24.8	52.2	25.4	17.1	1100
TiC <sub>p</sub> /Ni (Laser)	46.0	19.7	25.7	44.7	11.5	36.2	920
Ni		62.0	38.0		79.3	20.7	
Ni/(TiC <sub>p</sub> /Ni)	40.6	38.2	13.8	46.2	32.4	20.9	1000
Ni/(TiC <sub>p</sub> /Ni)/Ni	15.4	68.1	13.9	8.1	71.1	20.6	500

substrate interface. This is in agreement with previous studies of EDS cermet coatings. For example, Agarwal et al. demonstrated that the ESD TiB<sub>2</sub>/Ni coating on copper showed interfacial decohesion and crack formation, whereas a coherent and crack-free TiB<sub>2</sub>/Ni composite coating could be obtained on steel substrate [1]. When the molten droplets of TiC<sub>p</sub>/Ni were deposited onto the cold copper alloy substrate, they rapidly solidified to form a coating with a splash characteristic due to much greater thermal sink by the substrate. As a result, tensile thermal stress developed during cooling and solidification due to constriction of the droplets. The tensile thermal stress increased during deposition, causing cracking of coating and delamination at the weakly bonded interface. On the other hand, low toughness of the coating also facilitated the cracking within the TiC<sub>p</sub>/Ni coating.

In an attempt to improve the coating quality, laser treatment was carried out on the as-coated TiC<sub>p</sub>/Ni coating. Fig. 5 shows the SEM topography, cross-section and EDX element maps of the coating after laser scanning under the condition of 4 kW power and 80 mm/min speed. It was interesting to note that the coating became dense and free of cracks both within the coating and at the interface after laser scanning. A higher Cu content

was detected within the TiC<sub>p</sub>/Ni coating (Table 2). In addition, it was found that the Cu alloy substrate was slightly melted and penetrated into the cracks to seal them (Fig. 6). The laser scanning speed was sensitive, i.e. a faster speed of more than 100 mm/min could not result in significant change of the coating, whereas a slower speed of 60 mm/min would cause much melting of copper substrate.

### 3.2. Microstructural characterization of Ni/(TiC<sub>p</sub>/Ni)/Ni coating

In order to reduce or even eventually eliminate the cracks formed within the monolithic TiC<sub>p</sub>/Ni coating and at the interface when TiC<sub>p</sub>/Ni was deposited onto the copper substrate, another effort was made by using a multi-layer coating process that employed pure metallic Ni rod and TiC<sub>p</sub>/Ni rod as coating electrodes alternately during ESD depositions. This idea arose from the observation that Cu is not a good binder for TiC cermet while Ni is [16,17]. During this process, pure Ni was first coated onto the electrode surface as a barrier interlayer to reduce the Cu content that could be mixed into the TiC<sub>p</sub>/Ni coating during subsequent deposition using the TiC<sub>p</sub>/Ni rod. As shown in Fig. 7, the topography and cross-section images after deposition of Ni demonstrated a dense interface and no cracks in the Ni coating. The thickness of the Ni coating was approximately 25 μm. In addition, a smoother and uniform Ni coating with smaller droplets was produced in comparison with TiC<sub>p</sub>/Ni rough surface. The Ni was deposited in argon to prevent Ni from oxidation during deposition which ionizes easily, producing a plasma of relatively low thermal conductivity that tends to produce a fine spray of molten materials [5]. When TiC<sub>p</sub>/Ni was coated onto the Ni layer, a dense interface without delamination was obtained, but a few cracks in the vertical direction were still found within the coating (Fig. 8). It was also noted that TiC<sub>p</sub>/Ni mixed well with Ni coating during

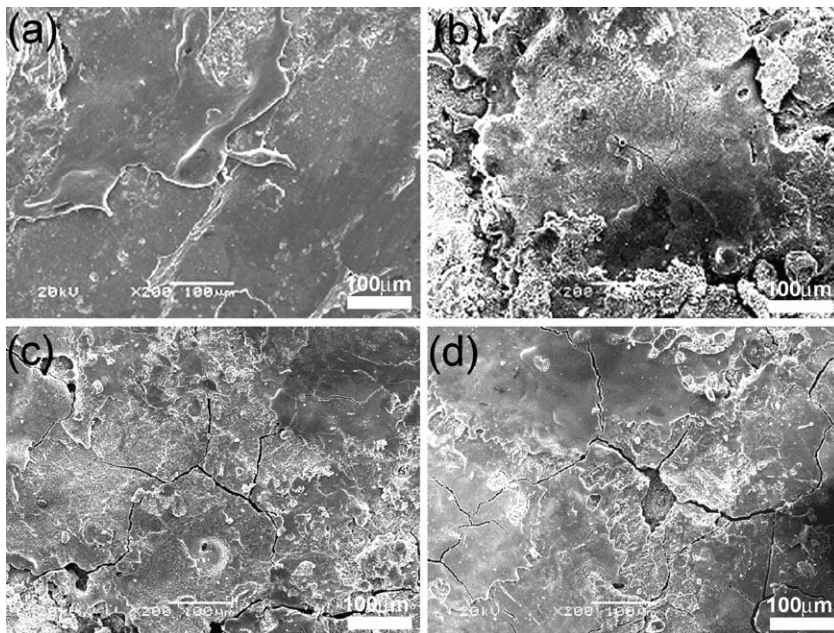


Fig. 4. Surface morphologies of monolithic TiC<sub>p</sub>/Ni coating deposited with 0.5 s (a), 2 s (b), 3 s (c) and 10 s (d), showing the cracking process during deposition.

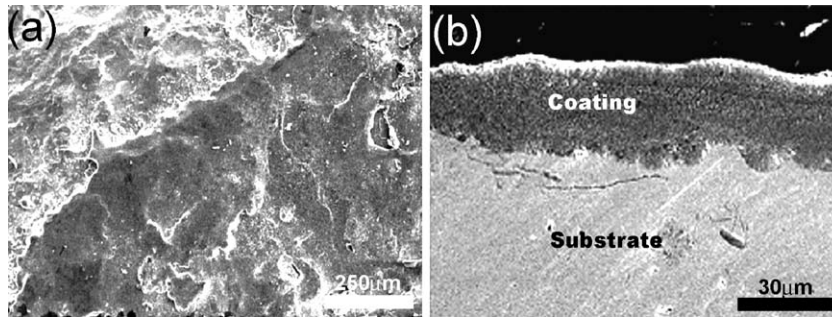


Fig. 5. Surface morphology (a) as well as cross-section image (b) of laser treated monolithic  $\text{TiC}_p/\text{Ni}$  coating.

deposition, resulting in a new  $\text{TiC}_p/\text{Ni}$  coating with higher Ni content and lower TiC content (Table 2). Relatively pure Ni was observed only at the interfacial region as shown in Fig. 8(d). The thickness of the whole coating  $\text{Ni}/(\text{TiC}_p/\text{Ni})$  increased somewhat ( $\sim 30 \mu\text{m}$ ), compared to the thickness of the Ni coating alone ( $25 \mu\text{m}$ ). On the other hand, the ratio of Ni content to Cu content in the  $\text{Ni}/(\text{TiC}_p/\text{Ni})$  coating increased due to the presence of the Ni (Cu) barrier interlayer (Table 2). Continuing coating with Ni rod on the top surface of  $\text{Ni}/(\text{TiC}_p/\text{Ni})$  coating resulted in a significant reduction in Ti content and an increase in Ni content due to mixing of Ni with the  $\text{Ni}/(\text{TiC}_p/\text{Ni})$  coating (Table 2). In addition, it was found that the vertical cracks

shown in Fig. 8 in the composite layer were eliminated after deposition of top Ni layer, as shown in Fig. 9.

XRD patterns, as shown in Fig. 10, indicated the main constituent phases of monolithic  $\text{TiC}_p/\text{Ni}$  coating and multi-Ni/ $(\text{TiC}_p/\text{Ni})/\text{Ni}$  coating were TiC, Ni and Cu. There were no discernible peaks from any other Ti–Cu or Ti–Ni intermetallic phases, showing mixing was purely physical in nature with Cu and Ni acting as binders. Consistent with the EDX results, Fig. 10 shows that the  $\text{Ni}/(\text{TiC}_p/\text{Ni})/\text{Ni}$  coating contained more Ni and less TiC, comparing to the monolithic  $\text{TiC}_p/\text{Ni}$  coating.

As mentioned above, during deposition of monolithic  $\text{TiC}_p/\text{Ni}$ , Cu up to 17 wt.% was physically mixed into the coating. In view of these observations, Cu mixed into the coating acted as a binder similar to Ni in the TiC–Ni cermet system. However, it should be noted that Ni acts an excellent binder, while Cu is not a suitable binder for a hard ceramic like TiC [1]. The role of Ni as an excellent binder for Ti based hard ceramics has been shown experimentally in various studies [16–18]. The difference of Cu and Ni as binders for ceramics can be explained from the point of view of their wetting characteristics. It has been reported that addition of Ni to TiC–Cu can increase wettability between Cu and TiC particulates and also improves the melting behavior of Cu by formation of Cu–Ni solution [19]. In addition, the wetting phenomenon has also been attributed to unfilled d orbitals in transition metals and their compounds, including carbides [20]. Based on the model proposed by Friedel [21], Cu is a poor binder for TiC because Cu has completely filled the d subshell electrons, while transition metals Ni, Fe and Co are excellent binder since they have unfilled d subshell electrons, i.e. 6 d subshell electrons. As a result, weak interface and low toughness of the monolithic  $\text{TiC}_p/\text{Ni}$  coating caused delamination and cracking under tensile thermal stress.

On the contrary, in the case of multi-layer  $\text{Ni}/(\text{TiC}_p/\text{Ni})/\text{Ni}$  coating, i.e.  $\text{TiC}_p/\text{Ni}$  deposited on the Ni interlayer, a strong interface between  $\text{TiC}_p/\text{Ni}$  and Ni(Cu) layer was formed (Figs. 8 and 9). The formation of a metallurgical bond depends on the chemical reaction or intermixing of two species at the interface. Although Ni did not show any chemical reaction with TiC during deposition, it was found that increased Ni content presents in the  $\text{Ni}/(\text{TiC}_p/\text{Ni})$  coating (Table 2) resulted in a strong interface, although Cu content was a little higher than in the monolithic  $\text{TiC}_p/\text{Ni}$  coating due to mixing of Cu from Ni (Cu) layer. Furthermore, deposition of Ni again as a top layer

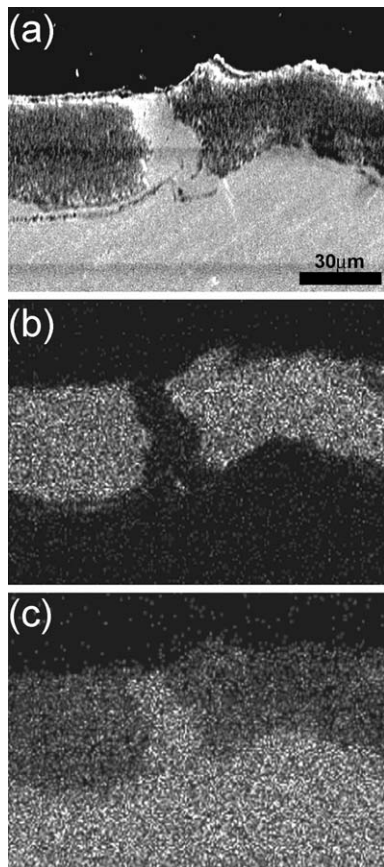


Fig. 6. SEM cross-section image (a) and element mapping of Ti  $K_\alpha$  (b) and Cu  $K_\alpha$  (c) of laser treated monolithic  $\text{TiC}_p/\text{Ni}$  coating, showing penetration of Cu into a crack.

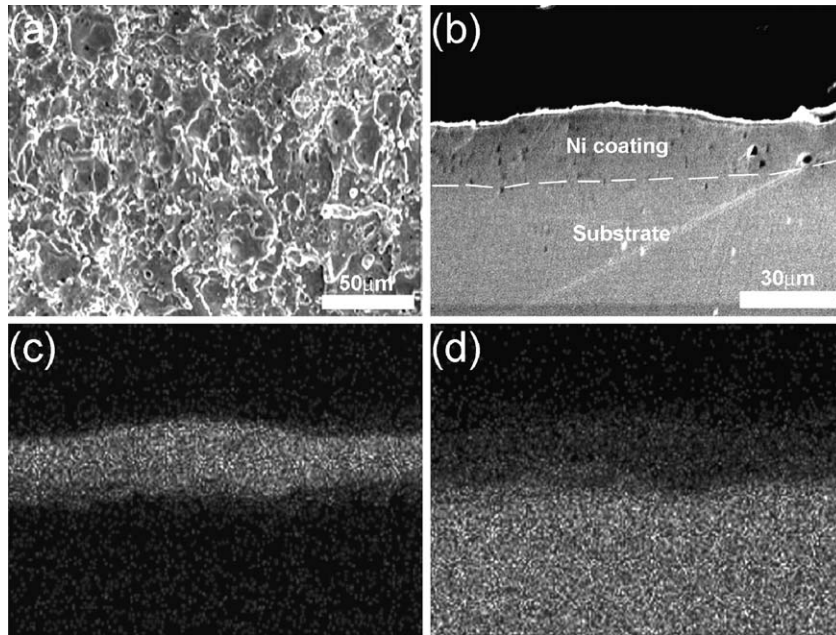


Fig. 7. Surface morphology (a) as well as cross-section image (b) and element mapping of Ni  $K_{\alpha}$  (c) and Cu  $K_{\alpha}$  (d) of Ni interlayer (as indicated by dashed lines).

onto Ni/(TiC<sub>p</sub>/Ni) coating further increased the Ni content in the coating (Table 2), leading to an increase in the toughness of the Ni/(TiC<sub>p</sub>/Ni)/Ni coating, similar to the behavior of the WC–Co system. As a result, a dense composite coating without cracks was obtained, which showed a hardness of ~HV500 and was strongly adherent to the copper alloy electrode substrate.

On the other hand, in the ESD process, the residual stress in the coating is always tensile, because the bulk of the substrate is cool, while the newly applied layer is ‘hot’. Parkansky et al. investigated the build-up of residual tensile stress during the ESD process [6]. They demonstrated that both residual tensile

stress and mass gain (thickness) increased with coating time, and that the predominant stress relief and surface damage mechanism for a brittle coating is surface cracking. In the present work, for the multi-layer deposition process, residual tensile stress developed during the coating process could be relieved by plastic deformation of the deposited Ni interlayer, similar to the case of ceramics-to-metals joining with a plastic metal interlayer [22,23].

It was noted that the laser-treated monolithic TiC<sub>p</sub>/Ni coating, which contained more Cu (~36 wt.%) than the coating before treatment (~17 wt.%) and hence a lower ratio of Ni

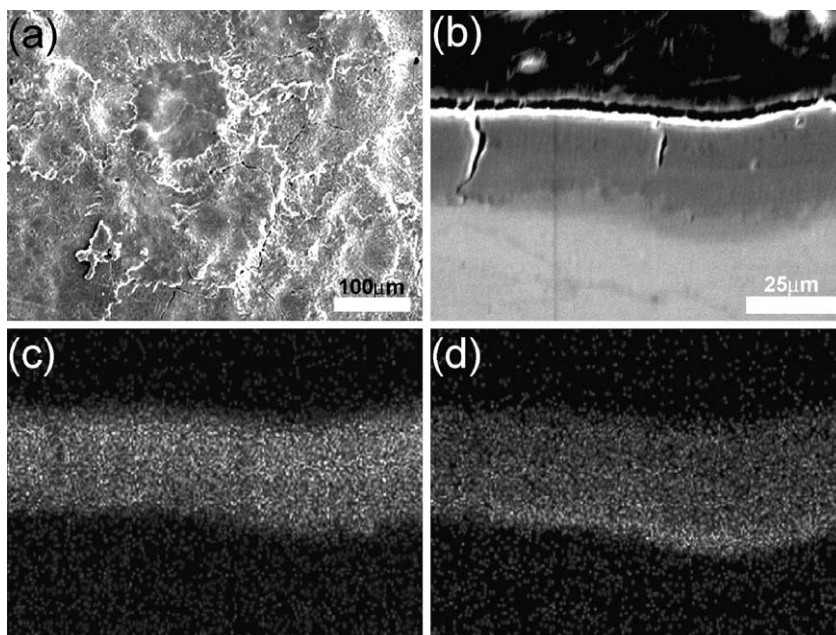


Fig. 8. Surface morphology (a) as well as cross-section image (b) and element mapping of Ti  $K_{\alpha}$  (c) and Ni  $K_{\alpha}$  (d) of multi-layer Ni/(TiC<sub>p</sub>/Ni) coating.

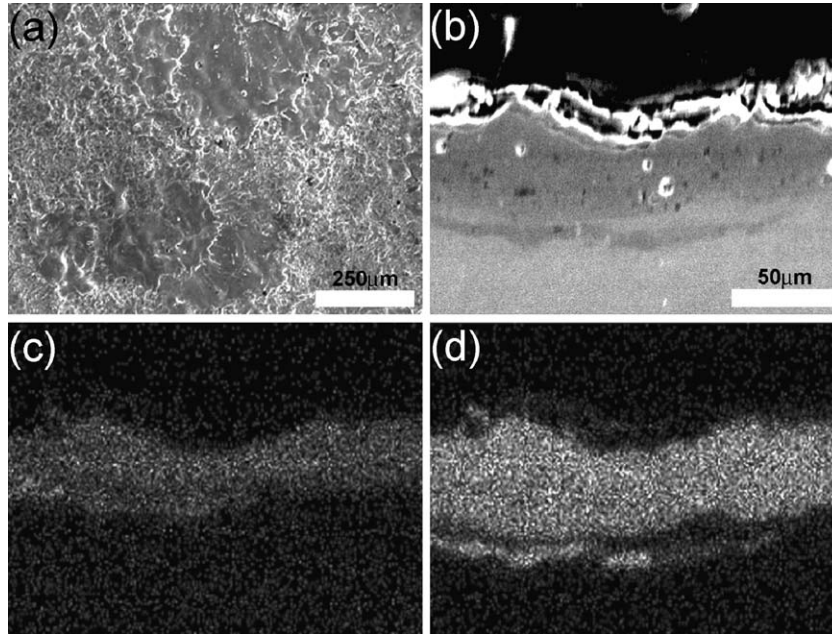


Fig. 9. Surface morphology (a) as well as cross-section image (b) and element mapping of Ti  $K_{\alpha}$  (c) and Ni  $K_{\alpha}$  (d) of multi-layer Ni/(TiC<sub>p</sub>/Ni)/Ni coating.

content to Cu content, did not show any cracking and delamination, whereas as-coated TiC<sub>p</sub>/Ni coating revealed much cracking. Mixing of Cu into TiC<sub>p</sub>/Ni might reduce the toughness of the coating due to its poor binder characteristics, but at the same time, may also increases the toughness because of the increased volume of high ductility Cu–Ni alloy matrix. Nevertheless, tensile stress is the direct driving force of cracking. During laser treatment, except for the melting of TiC<sub>p</sub>/Ni coating and a part of Cu alloy substrate near the top surface (Figs. 5 and 6), the whole electrode was also heated to high temperature since the energy density input of the laser was significantly higher than that of ESD [2]. As a result, cooling rate of the coating and substrate after laser scanning was much slower than in the case of ESD. Consequently, the tensile stress

developed within the coating decreased owing to laser scanning, resulting in freedom from cracks and delamination after cooling to room temperature.

3.3. Mechanical characterization

The mechanical behavior of the coatings was characterized by measurement of micro-hardness. Among all the coatings, as listed in Table 2, monolithic TiC<sub>p</sub>/Ni coating showed highest hardness (~HV 1100). Multi-Ni/(TiC<sub>p</sub>/Ni)/Ni coating presented the lowest hardness around HV 500, however, this hardness value was still much harder than the uncoated copper alloy electrode (HV 180). Laser treatment also reduced the hardness of TiC<sub>p</sub>/Ni coating due to the extensive mixing of Cu into the coating. Fig. 11 shows the distribution of hardness from

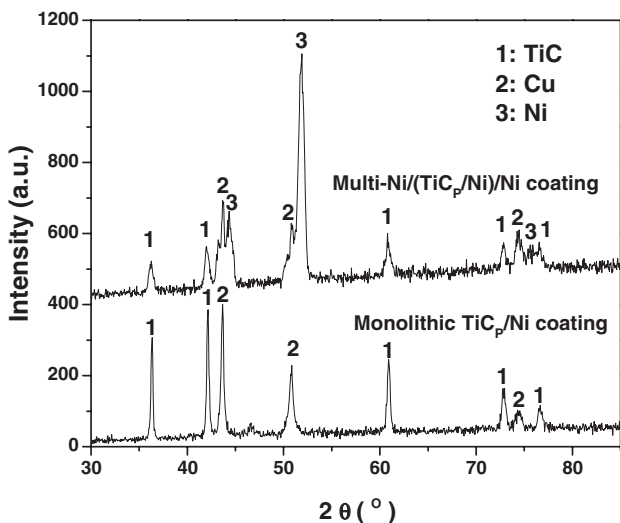


Fig. 10. XRD patterns taken from electrodes with monolithic TiC<sub>p</sub>/Ni coating and multi-layer Ni/(TiC<sub>p</sub>/Ni)/Ni coatings.

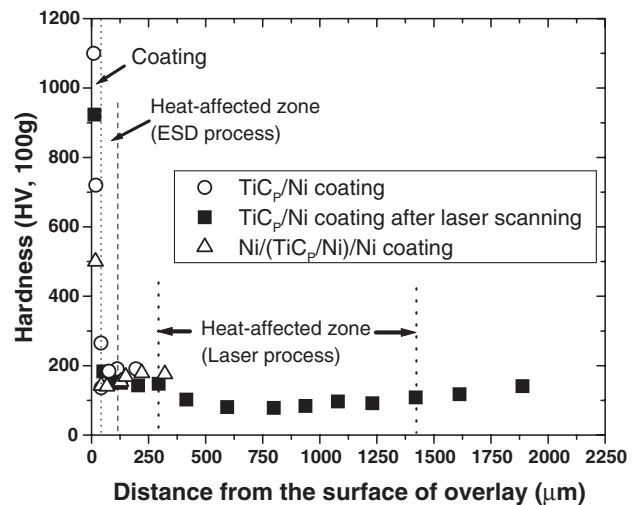


Fig. 11. Hardness distribution from the top surface of the coatings.

the top surface of the coatings. It was found that a narrow softened zone (heat-affected zone) was present within the substrate underneath the coating for ESD process. This is agreement with previous results [2], during the ESD process, some heat is added, raising the temperature of local spots on the electrode surface to melting point; however, the heat does not raise the temperature of the substrate high enough to melt it significantly or cause substantial microstructural changes. Also, the much greater thermal sink in the substrate, and the pulsed nature of the spark (the time between sparks is very long relative to the duration of the sparks themselves, thus allowing the substrate heat to dissipate rapidly) result in a transitory melting of the substrate and the formation of only a very small HAZ adjacent to the surface with a depth of about 60–100  $\mu\text{m}$  (Fig. 11). On the contrary, after laser scanning of as-coated  $\text{TiC}_p/\text{Ni}$  coated copper alloy electrode, a significant HAZ was formed, resulting in substantial softening of the substrate. It is known that a significant fraction of the laser beam coherent energy is consumed in interacting “directly” with the substrate, resulting in an intense rise in temperature of the substrate. A very small amount of laser beam energy is used in interaction with the environment above the substrate. Energy transfer is continuous during laser operation and relatively more efficient than in the ESD process, resulting in the formation of a large melt zone and a significant HAZ (Fig. 11). The softening of the copper alloy substrate as observed here will seriously reduce the mechanical stability of the welding electrode, thus limiting the applicability of laser treatment for increasing the soundness of welding electrode coatings.

#### 4. Conclusions

Deposition of monolithic  $\text{TiC}_p/\text{Ni}$  composite coating onto the surface of copper alloy electrode causes extensive cracking within the coating and delamination at the interface between the coating and substrate, due to high tensile thermal stress and low toughness of the coating. During multi-layer deposition of  $\text{Ni}/(\text{TiC}_p/\text{Ni})/\text{Ni}$ , although Ni does not react chemically with TiC, Ni acts as an excellent binder and may increase the toughness of the coating. Consequently, multi-layer deposition of  $\text{Ni}/(\text{TiC}_p/\text{Ni})/\text{Ni}$  produces dense coatings

and well bonded interface due to remarkably good mixing of Ni with the  $\text{TiC}_p/\text{Ni}$ . Post laser treatment of monolithic  $\text{TiC}_p/\text{Ni}$  coating could eliminate cracks and improve coating quality; however, the softening of the copper alloy substrate limits the usefulness of laser treatment for welding electrode coatings. The hardness of multi-layer  $\text{Ni}/(\text{TiC}_p/\text{Ni})/\text{Ni}$  coating is about HV 500, which is lower than that of monolithic  $\text{TiC}_p/\text{Ni}$  coating (HV 1000).

#### References

- [1] A. Agarwal, N.B. Dahotre, T.S. Sudarshan, Surf. Eng. 15 (1999) 27.
- [2] A. Agarwal, N.B. Dahotre, Mater. Charact. 42 (1999) 31.
- [3] Z. Li, W. Gao, P. Kwok, S. Li, Y. He, High Temp. Mater. Process. 19 (2000) 443.
- [4] R.N. Johnson, Thin Solid Films 118 (1984) 31.
- [5] R.N. Johnson, G.L. Sheldon, J. Vac. Sci. Technol., A, Vac. Surf. Films 4 (1986) 2740.
- [6] N. Parkansky, R.L. Boxman, S. Goldsmith, Surf. Coat. Technol. 61 (1993) 268.
- [7] I.V. Galinov, R.B. Luban, Surf. Coat. Technol. 79 (1996) 9.
- [8] A. Agarwal, N.B. Dahotre, Surf. Coat. Technol. 106 (1998) 242.
- [9] R.J. Wang, Y.Y. Qian, J. Liu, Appl. Surf. Sci. 228 (2004) 405.
- [10] S. Frangina, A. Masci, A. Di Bartolomeo, Surf. Coat. Technol. 149 (2002) 279.
- [11] S. Dong, Y. Zhou, Metall. Mater. Trans., A Phys. Metall. Mater. Sci. 34 (2003) 1501.
- [12] Y. Tanaka, M. Sakaguchi, H. Shirasawa, M. Miyahara, S. Normura, Int. J. Mater. Prod. Technol. 2 (1987) 64.
- [13] R. Holiday, J.D. Parker, N.T. Williams, Weld. World 37 (1996) 186.
- [14] J.D. Parker, N.T. Williams, R.J. Holiday, Sci. Technol. Weld. Join. 3 (1998) 65.
- [15] K.R. Chan, Y. Ding, S.J. Dong, Y. Zhou, Submitted for publication to the Welding J.
- [16] A.A. Ogwu, T.J. Davies, Scr. Mater. 40 (1999) 1377.
- [17] J. Zackrisson, A. Larsson, H.-O. Andren, Micron 32 (2001) 707.
- [18] H.J. Cai, X.-H. Zhang, J.V. Wood, Mater. Sci. Eng., A Struct. Mater.: Prop. Microstruct. Process. 280 (2000) 328.
- [19] L. Lu, J.Y.H. Fuh, Z.D. Chen, C.C. Leong, Y.S. Wong, Mater. Res. Bull. 35 (2000) 1555.
- [20] A.A. Ogwu, T.J. Davies, Mater. Sci. Technol. 9 (1993) 213.
- [21] J. Friedel, in: J.M. Ziman (Ed.), The Physics of Metals, Cambridge University Press, Cambridge, 1969.
- [22] Y. Zhou, K. Ikeuchi, T.H. North, Z. Wang, Metall. Mater. Trans., A Phys. Metall. Mater. Sci. 22 (1991) 2822.
- [23] Zheng Chen, M.S. Cao, Q.Z. Zhao, J.S. Zou, Mater. Sci. Eng. A Struct. Mater.: Prop. Microstruct. Process 380 (2004) 394.